Article

Mild Synthesis of a Family of Planar Triazinium Cations via Proton-Assisted Cyclization of Pyridyl Containing Azo Compounds and Studies on DNA Intercalation

M. Sinan, M. Panda, A. Ghosh, K. Dhara, P. E. Fanwick, D. J. Chattopadhyay, and S. Goswami

J. Am. Chem. Soc., **2008**, 130 (15), 5185-5193 • DOI: 10.1021/ja710211u • Publication Date (Web): 13 March 2008

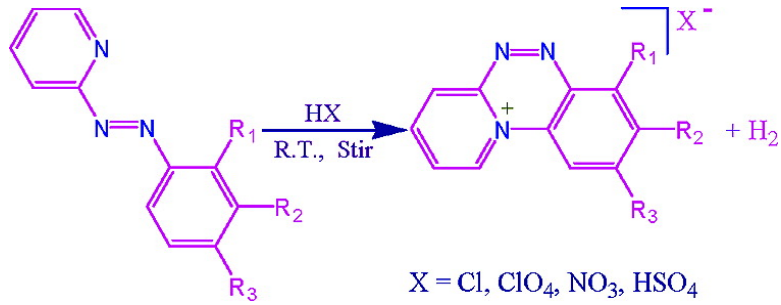

More About This Article

Additional resources and features associated with this article are available within the HTML version:

- Supporting Information
- Links to the 1 articles that cite this article, as of the time of this article download
- Access to high resolution figures
- Links to articles and content related to this article
- Copyright permission to reproduce figures and/or text from this article

View the Full Text HTML

J|A|C|S
ARTICLES

Published on Web 03/13/2008

Mild Synthesis of a Family of Planar Triazinium Cations via Proton-Assisted Cyclization of Pyridyl Containing Azo Compounds and Studies on DNA Intercalation

M. Sinan,[†] M. Panda,[†] A. Ghosh,[‡] K. Dhara,[†] P. E. Fanwick,[§] D. J. Chattopadhyay,[‡] and S. Goswami*[,†]

Department of Inorganic Chemistry, Indian Association for the Cultivation of Science, Kolkata 700 032, India, Department of Bio-Chemistry, University of Calcutta, Kolkata 700 019, India, and Department of Chemistry, Purdue University, West Lafayette, Indiana

Received November 10, 2007; E-mail: icsg@iacs.res.in

Abstract: An efficient synthesis of a family of heteroaromatic triazinium compounds, [**2a**]X−[**2g**]X (X= Cl, ClO_4, NO_3, and HSO_4), from 2-(arylazo)pyridines via proton-catalyzed heterocyclization is described. Characterization of the compounds is made by different spectroscopic, electrochemical techniques, as well as single-crystal structure determination of the triflate salt of a representative compound, [**2a**]CF_3SO_3. The bond parameters indicate that the tricyclo compound, **2a**$^+$, is planar and aromatic with a N−N bond length of 1.275(6) Å. These exhibited fluorescence with an emission maximum in the range of 540–535 nm with moderate quantum yields. The triazinium salts can be reduced in two successive one-electron steps as probed by cyclic voltammetry and coulometry. The paramagnetic radical intermediate **2a**$^\bullet$ is distinguished by a sharp and intense EPR spectrum. Fluorescence spectroscopy, circular dichroism, cyclic voltammetry, viscosity measurements, together with DNA melting studies have been used to characterize the binding of **2a**$^+$ with calf thymus DNA. The emission quenching of the compound by $[Fe(CN)_6]^{4-}$ decreased when bound to DNA. As determined by a MTT assay, **2a**$^+$ exhibited significant cytotoxicity at a higher concentration range of 1 mg/mL to 1 μg/mL; however, the % survival ratio increased with dilution. Cellular uptake studies of the referenced compound were followed by FACS analysis.

Introduction

Nitrogen containing heteroaromatic cations have been among the most researched kinds of organic compounds primarily because of their importance[1] in pharmaceutical and chemical industries. In fact, a large majority of these compounds are medicinally important,[2] and their motifs are found in many natural products.[3] In addition, these have also attracted attention in the fields as diverse[2,4] as DNA probes, fluorescent dyes, NLO materials, ionic liquids, and so on. Due to the multifaceted importance, several synthetic methodologies on the synthesis of such heterocyclic compounds have been developed during recent years.[5,6] A majority of the nitrogen heterocycles are prepared by condensation of a carbonyl function with a nitrogen nucleophile. Construction of heterocyclic rings via C−N bond formation by the combination of a nitrogen containing functional group and an arene, alkene, or alkane is also available.[7] Among the available syntheses, transition-metal-catalyzed[6] routes are attractive since these not only are straightforward but also can synthesize complicated molecules under mild conditions.

There has been a long-standing interest[8] in the coordination chemistry of 2-(arylazo)pyridine (abbreviated as 2-aap) ligands due to many reasons. The *trans*-isomer of 2-aap forms stable complexes with several d-block elements. Our recent work on these systems has revealed that the azo ligand, upon coordination, is susceptible to regioselective aromatic ring amination reaction via C−H functionalization.[9] On the other hand, the *cis*-isomer of 2-aap is unknown. However, molecular modeling of 2-aap has revealed that the pyridyl nitrogen, in its *cis* geometry,

[†] Indian Association for the Cultivation of Science.
[‡] University of Calcutta.
[§] Purdue University.

(1) Butler, M. S. *J. Nat. Prod.* **2004**, *67*, 2141.
(2) (a) Graves, D. E.; Velea, L. M. *Curr. Org. Chem.* **2000**, *4*, 915. (b) Bischoff, G.; Hoffmann, S.; Martínez, R.; Chacón-García, L. *Curr. Med. Chem.* **2002**, *9*, 321. (c) Martínez, R.; Chacón-García, L. *Curr.Med. Chem.* **2005**, *12*, 127.
(3) (a) Matia, M. P.; Ezaquerra, J.; García-Navío, J. L.; Vaquero, J. J.; Alvarez-Builla, J. *Tetrahedron Lett.* **1991**, *32*, 7575. (b) Hassner, A.; Murthy, K. S. K.; Maurya, R.; Dehaen, W.; Friedman, O. *J. Heterocycl. Chem.* **1994**, *31*, 687. (c) Lipińska, T. *Tetrahedron Lett.* **2002**, *43*, 9565.
(4) (a) Facchetti, A.; Abbotto, A.; Beverina, L.; van der Boom, M. E.; Dutta, P.; Evmenenko, G.; Marks, T. J.; Pagani, G. A. *Chem. Mater.* **2002**, *14*, 4996. (b) Mata, J. A.; Uriel, S.; Llusar, R.; Peris, E. *Organometallics* **2000**, *19*, 3797. (c) Seddon, K. R. *Nat. Mater.* **2003**, *2*, 363. (d) Welton, T. *Chem. Rev.* **1999**, *99*, 2071.
(5) (a) Padwa, A. *Prog. Heterocycl. Chem.* **1994**, *6*, 36. (b) Williams, G. D.; Wade, C. E.; Wills, M. *Chem. Commun.* **2005**, 4735. (c) Mills, A. D.; Nazer, M. Z.; Haddadin, M. J.; Kurth, M. J. *J. Org. Chem.* **2006**, *71*, 2687. (d) Yu, R. T.; Rovis, T. *J. Am. Chem. Soc.* **2006**, *128*, 2782.
(6) Nakamura, I.; Yamamoto, Y. *Chem. Rev.* **2004**, *104*, 2127.
(7) Tsang, W. C. P.; Zheng, N.; Buchwald, S. L. *J. Am. Chem. Soc.* **2005**, *127*, 14560.
(8) (a) Krause, R. A.; Krause, K. *Inorg. Chem.* **1980**, *19*, 2600. (b) Goswami, S.; Mukherjee, R. N.; Chakravorty, A. *Inorg. Chem.* **1983**, *22*, 2825. (c) Velders, A. H.; Kooijman, H.; Spek, A. L.; Haasnoot, J. G.; de Vos, D.; Reedijk, J. *Inorg. Chem.* **2000**, *39*, 2996. (d) Panda, M.; Das, C.; Lee, G.-H.; Peng, S.-M.; Goswami, S. *Dalton Trans.* **2004**, 2655.

Scheme 1

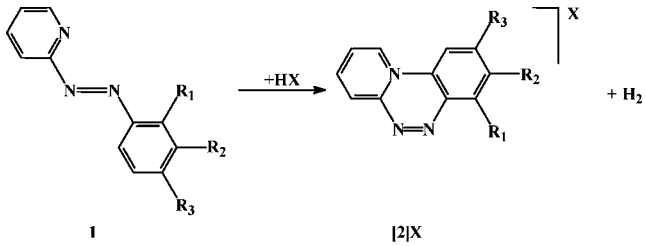

can be in bonding proximity to the *ortho*-carbon of the aryl ring. This arrangement, in principle, generates a possibility of ring closure reaction with a new C−N bond formation that results in the synthesis of cationic heteroaromatics.

In this paper, we introduce a proton-catalyzed, mild, and one-pot synthesis of salts of a novel family of planar triazinium salts, [**2a**]X−[**2g**]X (X = Cl, ClO_4, NO_3, HSO_4) from readily accessible *trans*-2-aap. The synthesis, to the best of our knowledge, is among the simplest ones of the available literature procedures for making cationic heterocyclic compounds. Literature search has revealed that 3-(phenylazo)pyridine in concentrated sulfuric acid (98%) undergoes photocyclization[10] with C−C bond formation analogous to photocyclization of certain azobenzenes to benzo[*c*]cinnoline derivatives.[11] It has been possible to isolate the different salts of the parent molecules by the use of common mineral acids as the proton source, and their characterization is made by different spectroscopic, electrochemical techniques, as well as single-crystal structure analysis of a representative compound. These studies, including NMR, EPR, and UV–visible spectra of the parent and eletrogenerated reduced compound, have allowed us to characterize the formation of stable radicals by the partial reduction of [**2**]X.

Since planarity and cationic character are the two desirable properties[2,12] for a compound to function as a DNA intercalator, we have also investigated the interactions of a representative compound with DNA. Effective binding of $\mathbf{2a}^+$ with DNA has been evidenced by a battery of complementary methods necessary to determine the binding modes of a compound to DNA. In the present context, it is worth noting that DNA is a target of many clinically important chemotherapeutic agents. These agents bind to DNA within the grooves, ordinarily within the minor rather than the major groove, and/or by intercalating between base pairs. An understanding of DNA−ligand interactions at the molecular level is thus important[13] for design of new drugs and probes that can recognize specific DNA sequences and structural motifs.

Results and Discussion

Synthesis. The stable *trans*-form of 2-(arylazo)pyridines (**1**) is used[14] for the synthesis of the triazinium salts. Schematic representation of the synthesis is shown in Scheme 1, and the isolated compounds are collected in Chart 1. The key feature

Chart 1

Compound	R_1	R_2	R_3	Yield (%)
[**2a**]Cl	H	H	H	65
[**2a**]ClO_4	H	H	H	62
[**2a**]NO_3	H	H	H	64
[**2a**]HSO_4	H	H	H	60
[**2b**]Cl	H	Me	H	62
[**2c**]Cl	H	H	Me	63
[**2d**]Cl	H	H	OMe	64
[**2e**]Cl	Cl	H	H	60
[**2f**]Cl	H	H	Cl	61
[**2g**]Cl	H	H	Br	64

of this method is the combination of C−H functionalization via protonation, *trans* to *cis* isomerization, and cyclization via C−N bond fusion.

Since *trans* → *cis* isomerization of the diazo compounds is usually a photo-driven process,[15] we began the study by irradiating the representative compound *trans*-2-(phenylazo)pyridine (2-pap) with UV light, which failed to produce any detectable *cis*-product. However, a similar reaction in the presence of dilute aqueous perchloric acid (0.01 M) in acetonitrile produced salt of the cationic triazinium ion [**2a**](ClO_4) in 62% yield. It was later found that the above reaction, even in dark, delivers the same compound in a comparable yield, indicating that the reference transformation occurs thermally. To have an insight about the nature of the intermediate of the reaction, the preformed protonated salt,[16] *trans*-[Hpap](ClO_4), was stirred in acetonitrile at room temperature. The reaction also resulted in the formation of the triazinium salt, [**2a**](ClO_4), in a similar yield (60%). It is thus concluded that the above chemical reaction is initiated via protonation of *trans*-2-aap.

To look for generalization, the reaction was successfully applied on several other substituted *trans*-2-aap compounds (Chart 1), which resulted in the formation of the expected triazinium ions $\mathbf{2b}^+$−$\mathbf{2g}^+$ in comparable yields. It is worth noting here that the 2-chloro-substituted compound, 2-[Cl-2-Haap], formed the 8-chloro-substituted triazinium salt, indicating that H_2 elimination is preferred over HCl elimination. Having been successful with $HClO_4$, we tried these reactions with other common mineral acids, which also produced the expected products in good yields (≥ 60%). Notably, the chloride ion is ubiquitous in physiological systems, and hence the chloride salts of these compounds are particularly useful in the studies of DNA interactions.

Formation of the compound $\mathbf{2}^+$ from **1** can be explained by invoking the following probable steps (Scheme 2). In presence of acid, protonation may occur on the azo nitrogen atoms and the pyridine ring nitrogen atom, as well.[16,17] Accordingly, the protonated species **A**, **B**, and **C** are expected to remain in equilibrium in different proportions. Among the different protonated forms, the form **C** is active for the conversion in success. The protonated form **C** causes the π-polarization in such a way that the *ortho*- and *para*-positions of the phenyl

(9) (a) Saha, A.; Ghosh, A. K.; Majumdar, P.; Mitra, K. N.; Mondal, S.; Rajak, K. K.; Falvello, L. R.; Goswami, S. *Organometallics* **1999**, *18*, 3772. (b) Das, C.; Saha, A.; Hung, C. -H; Lee, G.-H.; Peng, S.-M.; Goswami, S. *Inorg. Chem.* **2003**, *42*, 198.
(10) Barton, J. W.; Walker, R. B. *Tetrahedron Lett.* **1975**, *8*, 569.
(11) Jamieson, N. C.; Lewis, G. E. *Aust. J. Chem.* **1967**, *20*, 321.
(12) (a) Lerman, L. S. *J. Mol. Biol.* **1961**, *3*, 18. (b) Erkkila, K. E.; Odom, D. T.; Barton, J. K. *Chem. Rev.* **1999**, *99*, 2777.
(13) Zhang, L. Z.; Tang, G.-Q *J. Photochem. Photobiol. B* **2004**, *74*, 119.
(14) Campbell, N.; Henderson, A. W.; Taylor, D. *J. Chem. Soc.* **1953**, 1281.
(15) (a) Tamai, N.; Miyasaka, H. *Chem. Rev.* **2000**, *100*, 1875. (b) Nishihara, H. *Bull. Chem. Soc. Jpn.* **2004**, *77*, 407.
(16) Saha, A.; Das, C.; Goswami, S. *Indian J. Chem.* **2001**, *40A*, 198.
(17) Panneerselvam, K.; Hansongnern, K.; Rattanawit, N.; Liao, F.-L.; Lu, T.-H *Anal. Sci.* **2000**, *16*, 1107.

Scheme 2

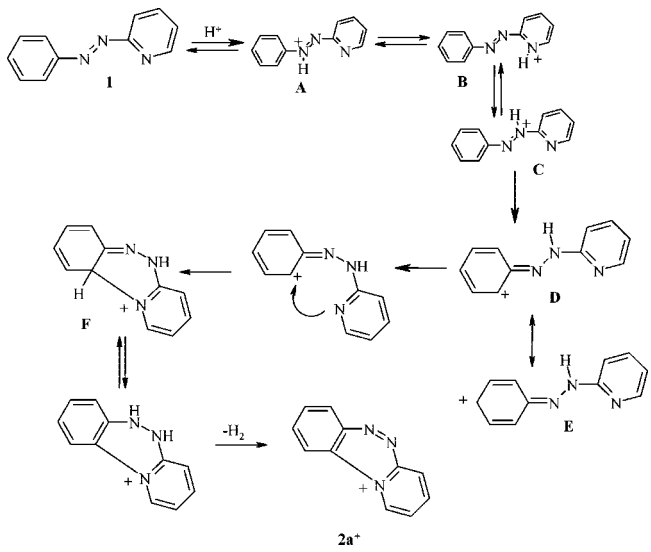

Table 1. Selected bond lengths (Å) of [**2a**]CF_3SO_3

C(1)−C(2)	1.359(6)	C(9)−C(10)	1.364(6)
C(2)−C(3)	1.387(6)	C(10)−C(11)	1.396(6)
C(3)−C(4)	1.372(6)	C(11)−C(12)	1.373(6)
C(4)−C(5)	1.379(6)	C(12)−C(13)	1.384(5)
C(5)−N(6)	1.387(5)	C(13)−C(8)	1.401(5)
N(6)−N(7)	1.275(6)	C(13)−N(14)	1.401(5)
N(7)−C(8)	1.387(5)	N(14)−C(1)	1.375(4)
C(8)−C(9)	1.393(6)	N(14)−C(5)	1.385(4)

ring become electron-deficient (**D** and **E**). The closely spaced pyridyl nitrogen in the *syn*-conformation subsequently attacks the electrophilic *ortho*-carbon of phenyl ring and leads to a tricyclic system **F**. Such nucleophilic character of the pyridine ring nitrogen is known[18] in the literature. The tautomeric shift of hydrogen followed by dehydrogenation of the hydrazo motif finally gives the salt of $\mathbf{2a}^+$ where all the rings are aromatic.

Characterization and X-ray Structure. Microanalytical, positive-ion ESI-mass spectra, together with ^{1}H NMR spectral data of the triazinium compounds, [**2a**]X−[**2g**]X, convincingly support their formulations as shown in Scheme 1. Characterization data are collected in the Experimental Section. NMR spectra of two representative triazinium compounds, [**2a**]Cl and [**2b**]Cl, are submitted as Supplementary Figures S1 and S2.

These triazinium salts are generally crystalline, and the compound [**2a**]CF_3SO_3formed X-ray quality crystals. X-ray structure of this compound further authenticates the formation of the above compound from a heretofore unknown chemical transformation. A molecular view of the cationic compound is shown in Figure 1, and an ORTEP of [**2a**]CF_3SO_3 is submitted as Supplementary Figure S3. The most significant observation in this structure is the planarity of the triazinium cation, with no atom deviating by more than 0.007 Å from the mean plane. The interatomic distances (Table 1) in it are normal and lie between a single and double bond lengths. Notably, the N−N length (1.275(6) Å) in [**2a**]CF_3SO_3 is appreciably longer than that (1.258(5) Å) observed in the protonated compound, *trans*-[Hpap]ClO_4.[16,17] All of this evidence together points to the aromatic nature of the compound.

(18) (a) Ghosh, K.; Sen, T.; Frohlich, R. *Tetrahedron Lett.* **2007**, *48*, 6308. (b) Skov, M.; Svete, J.; Stanovnik, B. *J. Heterocycl. Chem.* **2000**, *37*, 307. (c) Skov, M.; Svete, J.; Stanovnik, B. *Heterocycles* **2000**, *52*, 845. (d) Stanovnik, B.; Steve, J. *Chem. Rev.* **2004**, *104*, 2433.

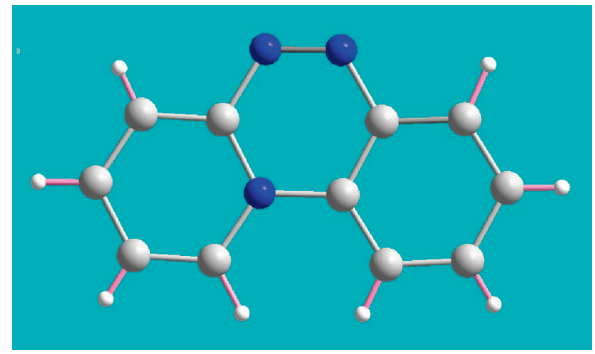

Figure 1. Molecular view of $\mathbf{2a}^+$. Color code: N (blue), C (gray), and H (white).

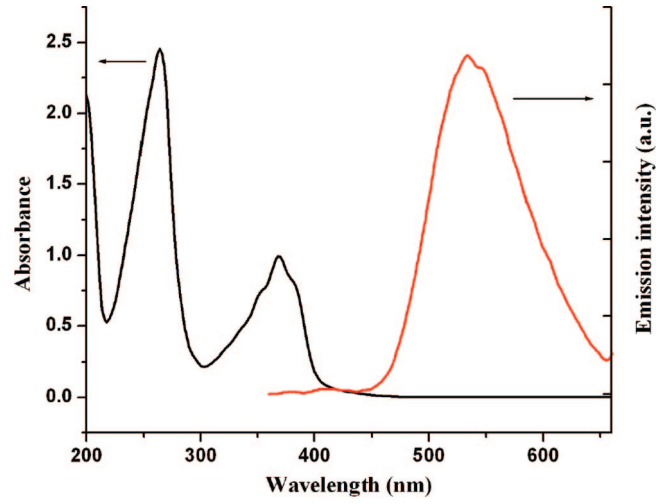

Figure 2. UV–vis (black) and emission (red) spectra of [**2f**]Cl in CH_3CN.

Optical Spectra. Absorption spectra of the triazinium salts [**2a**]X−[**2g**]X are characterized by an intense $\pi-\pi^*$ absorption band peaking near 260 nm and a relatively weak and broad $n-\pi^*$ band[19,20] near 350 nm. These compounds in acetonitrile exhibited fluorescence at room temperature upon excitation at 340 nm with emission maximum λ^{em} in the range of 535–540 nm and quantum yield in the range of 0.22−0.15. The lifetime of a representative [**2a**](ClO_4) at 298 K was found to be 3.90 ns. Absorption and emission spectra of [**2f**]Cl are shown in Figure 2. In contrast, the starting parent compounds *trans*-2-aap are not fluorescent. It is believed that the rigidity of the tricyclo triazinium salts causes reduction of loss of energy via a nonradiative relaxation pathway. An IR spectral feature of the triazinium salts is qualitatively different from that of the parent compound, *trans*-2-aap. For example, the $\nu_{N=N}$ stretching frequencies in the parent compound[16] (ca. 1425 cm^{-1}) are shifted to lower frequencies in [**2a**]X by around 80 cm^{-1} due to significant elongation of the N−N length. Optical spectral data of the compounds are collected in Table 2.

Redox Properties. Redox behavior of the triazinium compounds was examined generally in acetonitrile by cyclic voltammetry. However, the study of the unsubstituted compound

(19) The absorbption bands are structured, which can be attributed to vibronic fine structures arising from the skeletal vibrations[20] of the aromatic core.

(20) Otsuki, J.; Suwa, K.; Narutaki, K.; Sinha, C. R.; Yoshikawa, I.; Araki, K. *J. Phys. Chem. A* **2005**, *109*, 8064.

Table 2. IR, UV–vis, and Emission Spectral Data

compound	IR[a], cm^{-1} $\nu_{C=C} + \nu_{C=N}$	IR[a], cm^{-1} $\nu_{N=N}$	absorption[b] λ_{max}, nm (ϵ, M^{-1} cm^{-1})	λ_{em},[b] nm ($\lambda_{ex,nm}$)
[**2a**]Cl	1605	1360	375[c](5155), 359(7915), 346[c](7720), 259(22980)	536(340)
[**2a**]ClO_4	1605	1365	375[c](5320), 359(8160), 348[c](7930), 258(23520)	535(340)
[**2a**]NO_3	1600	*d*	376[c](5320), 359(8345), 346[c](5320), 259(24750)	534(340)
[**2b**]Cl	1595	1370	372[c](5745), 352(6775), 278(23590)	535(340)
[**2c**]Cl	1610	1355	384[c](5180), 368(5965), 351[c](5180), 262(18680)	535(340)
[**2d**]Cl	1610	1355	408(8295), 393[c](7840), 303(3035), 266(10570), 258(10585), 240(9180)	508(400)
[**2e**]Cl	1595	1348	375(7180), 360(7180), 346[c](6155), 287(10350), 258(11475), 248(11670)	548(340)
[**2f**]Cl	1600	1350	380[c](8605), 368(10440), 353[c](7830), 264(25805)	535(340)
[**2g**]Cl	1595	1350	385(9660), 371(11695), 355(8395), 267(26190)	535(340)

[a] In KBr disk. [b] In acetonitrile. [c] Shoulder. [d] Overlapped with $\nu_{NO_3^-}$ frequencies.

Table 3. Cyclic Voltammetry Data[a]

compound	Reduction(*i*)$E_{1/2}$, V (ΔE_p, mV)[b]	Reduction(*ii*)E^c (V)
[**2a**]Cl	−0.26(80)	−1.11
[**2a**]ClO_4	−0.26(80)	−1.10
[**2a**]NO_3	−0.18(80)	−1.26
[**2b**]Cl	−0.29(80)	−1.17
[**2c**]Cl	−0.31(90)	−0.95
[**2d**]Cl	−0.38(60)	−1.23
[**2e**]Cl	−0.14(80)	−1.06
[**2f**]Cl	−0.17(80)	−1.12
[**2g**]Cl	−0.16(90)	−1.12

[a] In acetonitrile solution, supporting electrolyte Et_4NClO_4 (0.1 M), reference electrode SCE. [b] $E_{1/2} = 0.5(E_{pa} + E_{pc})$, where E_{pa} and E_{pc} are anodic and cathodic peak potentials respectively, $\Delta E_p = E_{pa} - E_{pc}$ scan rate = 50 mV s^{-1}. [c] Irreversible, cathodic peak potential.

[**2a**]Cl was also carried out in aqueous Tris buffer (cf. studies of DNA interactions). The compound [**2a**]Cl showed a reversible reduction wave at –0.26 V and an irreversible cathodic response at –1.10 V versus SCE (Supplementary Figure S4). Since the second response is irreversible, we do not consider it further. The redox potentials are found to be sensitive to the nature of substitutions on the compounds. Thus a gradual shift of reduction potentials to more negative values was observed (Table 3) on moving from the compounds containing an electron-withdrawing substituent, such as Cl (−0.17 V), to an electron-donating substituent, such as OCH_3 (−0.38 V). A plot of redox potentials of these compounds versus σ [σ = Hammett substitution constant] is found to be excellently linear with the reaction constant, 0.3 V. Segmented cyclic voltammograms of the three compounds, viz. [**2a**]Cl, [**2d**]Cl, and [**2f**]Cl, are displayed in Figure 3, and a Hammett's plot for [**2a**]Cl−[**2g**]Cl is submitted as Supplementary Figure S5. Two one-electron reductions of $\mathbf{2}^+$ imply the formation of the radical $\mathbf{2}^\bullet$ and the anion $\mathbf{2}^-$, successively (eq 1)).

$$2^+ \underset{-e}{\overset{+e}{\rightleftharpoons}} 2^\bullet \overset{+e}{\longrightarrow} 2^- \qquad (1)$$

To have further insight into the redox processes, constant potential exhaustive electrolysis of the representative compound [**2a**]Cl was performed at −0.5 V. The yellow orange solution of $\mathbf{2a}^+$ became brown upon reduction, and the coulomb count corresponded to one-electron transfer. The original compound was completely regenerated by reoxidation of the reduced compound at 0.0 V, suggesting that the redox process

$$2^+ \underset{-e}{\overset{+e}{\rightleftharpoons}} 2^\bullet$$

is chemically reversible. The electrolytically reduced compound, $\mathbf{2a}^\bullet$, showed a single line sharp EPR spectrum at *g*, 2.001 (Figure 4), characterizing the formation of the free radical. Notably, the compounds can also be reduced chemically by an aqueous solution of sodium dithionite. It may be relevant to note here that the vast majority of organic radicals are transient[21] and highly reactive. In contrast, the present triazene radical $\mathbf{2a}^\bullet$ is quite stable in a deareated solution. Its stability is attributed to electron delocalization over the conjugated triazene ring.

Studies of DNA−$\mathbf{2a}^+$ Interactions. Since many cationic heterocycles are well-documented for their medicinal activities, we have undertaken the studies to explore the possible interactions of the reference triazinium compounds with DNA. The compounds are freely soluble in aqueous Tris buffer, and the experiments were performed at pH 7.2. In this paper, we have confined ourselves only to the studies of the nature of interactions between DNA and the unsubstituted compound [**2a**]Cl. The interactions between DNA and [**2a**]Cl were primarily established using agarose gel electrophoresis technique. The compound interacts both with linear and circular DNA, and the fluorescence emission intensity was found to be DNA concentration dependent. Notably, the compound, $\mathbf{2a}^+$, is found to be sensitive, and as small as 60 ng of linear ds-DNA could be visualized under trans-illuminator (Supplementary Figure S6).

Luminescence Studies. The results of the emission titration of [**2a**]Cl with CT DNA are illustrated in Figure 5, and the Stern−Volmer plot of quenching is shown as an inset. Upon addition of DNA, the emission intensities of $\mathbf{2a}^+$ decreased steadily nearly by 25%. The quenching was saturated when DNA concentration exceeded 15 times that of the triazinium salt, [**2a**]Cl. This emission quenching phenomenon reflects the changes of excited-state electronic structure as a consequence of the electronic interactions in the $\mathbf{2a}^+$−DNA complexes. The fluorescence quenching constant evaluated using Stern−Volmer's (SV) equation (eq 3, cf. Experimental Section) is 1.3×10^3 M^{-1}. Similar fluorescence quenching was noted before with other known DNA intercalators[13,22] such as (9-anthrylmethyl)ammonium chloride (AMAC), methylene blue, daunomycin, etc.

The relative binding of $\mathbf{2a}^+$ to CT DNA (K_{app}) was measured monitoring the emission intensity of ethidium bromide (EB) as

(21) (a) Griller, D.; Ingold, K. U. *Acc. Chem. Res.* **1976**, *9*, 13. (b) Hicks, R. G.; Hooper, R *Inorg. Chem.* **1999**, *38*, 284. (c) Lalevée, J.; Allonas, X.; Fouassier, J. P. *J. Org. Chem.* **2006**, *71*, 9723.
(22) (a) Kumar, C. V.; Asuncion, E. H. *J. Am. Chem. Soc.* **1993**, *115*, 8547. (b) Chaires, J. B.; Dattagupta, N.; Crothers, D. M. *Biochemistry* **1982**, *21*, 3933.

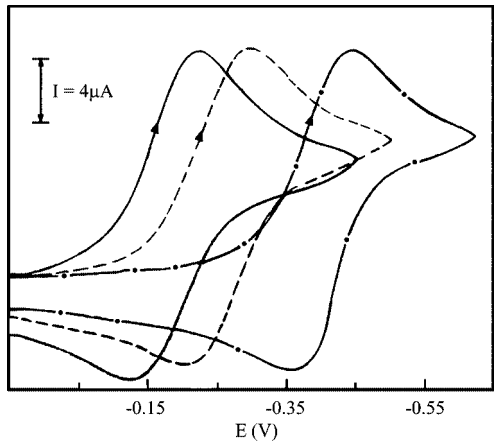

Figure 3. Segmented voltammograms of [**2f**]Cl (—), [**2a**]Cl (- - -), and [**2d**]Cl (- • -) in CH_3CN.

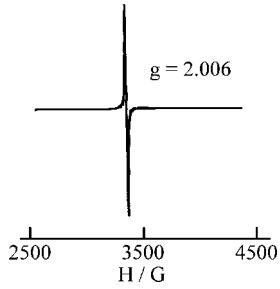

Figure 4. EPR spectrum of electrogenerated **2a** at 120 K.

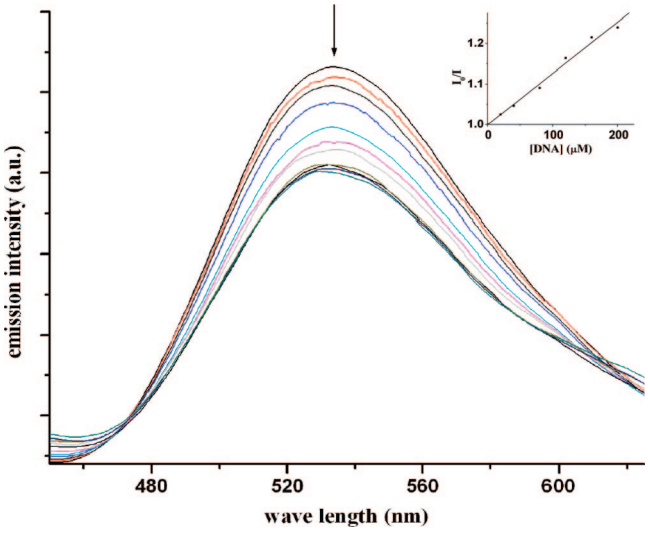

Figure 5. Emission spectra of $\mathbf{2a}^+$ (20 μM) in Tris-HCl, 50 mM NaCl buffer in the absence and presence of increasing amount of DNA (20−360 μM). Inset: SV plot for quenching.

a spectral probe[23] (Supplementary Figure S7) and following[24] eq 2

$$K_{EB}[EB] = K_{app}[\mathbf{2a}^+] \quad (2)$$

where K_{EB} is 1.0×10^7 M^{-1}, the concentration of EB is 1.3 μM, and the concentration of $\mathbf{2a}^+$ is that used to obtain a 50%

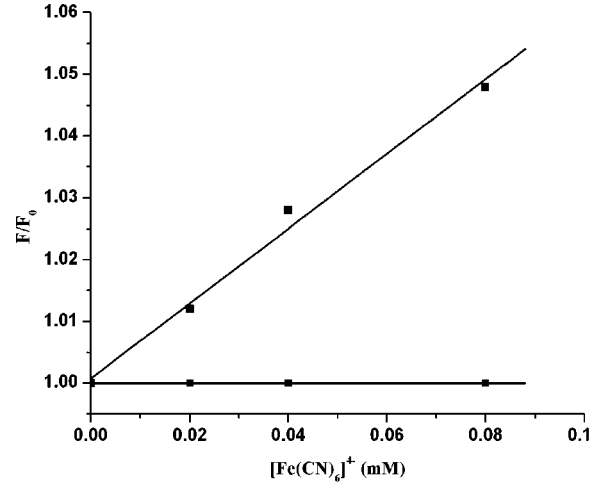

Figure 6. Emission quenching curve of [**2b**]Cl in the absence of DNA and in the presence of DNA with increasing concentration of the quencher $[Fe(CN)_6]^{4-}$. [[**2b**]Cl = 20 M, [DNA] = 200 M].

reduction of fluorescence intensity of EB. DNA-bound EB shows a strong emission $\lambda_{max} = 600$ nm upon excitation at 510 nm. The reference triazinium compound does not show detectable emission in this region (cf. spectra). Gradual addition of $\mathbf{2a}^+$ to DNA-bound EB results in reduction of emission intensities due to displacement of EB by $\mathbf{2a}^+$. Notably, EB, in its free state, is nearly nonemissive. The value of K_{app} evaluated as above is 2.6×10^4 M^{-1}.

Steady-state emission quenching experiments using $K_4[Fe(CN)_6]$ as a quencher were also investigated.[25] In the absence of DNA, [**2a**]Cl was efficiently quenched by $[Fe(CN)_6]^{4-}$ following a linear SV plot (Figure 6) with a slope of 0.60 mM^{-1}. In contrast, emission quenching of [**2a**]Cl, in the presence of DNA, was negligible. The fact that no quenching seems to be observed when the fluorophore is bound to DNA is striking and indicates very good protection[26] against the ferrocyanide quencher and that this situation is consistent with DNA intercalation.

DNA Melting Study. Gradual addition of CT DNA to the triazinium salt unfortunately failed to produce any noticeable change of the nature of UV–visible absorption spectra of [**2a**]Cl. However, strong evidence for the interaction of $\mathbf{2a}^+$ into the DNA helix was obtained from the DNA melting studies. Intercalation of small molecules is known to increase the helix melting temperature,[22a,27] the temperature at which the double helix denatures into single-stranded DNA. The DNA melting curves for CT DNA in the absence and presence of the triazinium compound are submitted as Supplementary Figure S8. Compared to untreated DNA ($T_m = 72.5$ °C), the melting temperature of the complexed DNA increased to 79 °C.

CV of DNA-Bound $\mathbf{2a}^+$. The fact that the triazinium salt, [**2a**]Cl, undergoes reduction reversibly in acetonitrile to produce a stable free radical (cf. Redox Properties) prompted us to study effects of DNA interaction on the cyclic voltammetry of $\mathbf{2a}^+$. Cyclic voltammetric profiles of the free cation as well as its DNA-bound state are shown in Figure 7. The compound in Tris-

(23) (a) Waring, M. J. *J. Mol. Biol.* **1965**, *13*, 269. (b) Le Pecq, J, -B.; Paoletti, *J. Mol. Biol.* **1967**, *27*, 87.
(24) Lee, M.; Rhodes, A. L.; Wyatt, M. D.; Forror, S.; Hartley, J. A. *Biochemistry* **1993**, *32*, 4237.
(25) Kumar, C. V.; Barton, J. K.; Turro, N. J. *J. Am. Chem. Soc.* **1985**, *107*, 5518.
(26) (a) Liu, F.; Wang, K.; Bai, G.; Zhang, Y.; Gao, L. *Inorg. Chem.* **2004**, *43*, 1799. (b) Wu, J. Z.; Yuam, L.; Wu, J. F. *J. Inorg. Biochem.* **2005**, *99*, 2211.
(27) (a) Patel, D. J. *Acc. Chem. Res.* **1979**, *12*, 118. (b) Patel, D. J.; Canuel, L. L. *Proc. Natl. Acad. Sci. U.S.A.* **1976**, *73*, 3343.

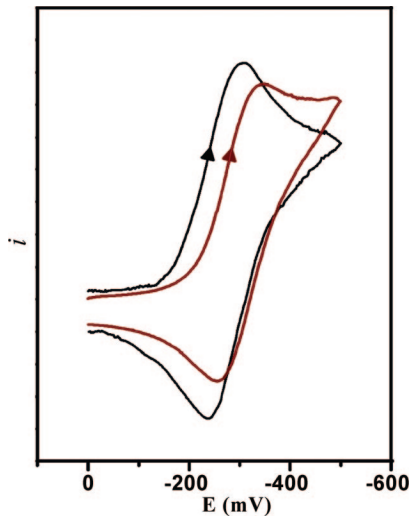

Figure 7. Cyclic voltammograms of unbound [**2a**]Cl (black) and [**2a**]Cl in presence of CT DNA (red) in Tris-HCl, 50 mM NaCl solution at r = 15.

HCl 50 mM NaCl (pH 7.2) displayed a reversible voltammogram with $E_{1/2} = -0.28$ V versus SCE with $\Delta E_p = 75$ mV for the couple

$$2^+ \underset{-e}{\overset{+e}{\rightleftharpoons}} 2^\bullet$$

For comparison, the value of $E_{1/2}$ in acetonitrile is –0.26 (vide supra). In the presence of CT DNA at the same concentration of **2a**$^+$, both the anodic and cathodic peak potentials shifted to more negative values versus a solution without DNA. The value of ΔE_p in the DNA-bound state was 85 mV, showing that reversibility of the electron transfer[28] process was still maintained under this condition, but the $E_{1/2}$ value was shifted to more negative potential by 20 mV. The related cationic DNA intercalators such as EtBr and proflavine undergo irreversible reduction(s)[29] without any anodic counterpart due to instabilities of the corresponding radicals. Thus exciting applications of the present triazinium binder and the related compounds in probing oxidative DNA cleavage may be anticipated.

Circular Dichroic Spectra. To have an insight into the conformational changes to the helix of DNA due to binding, the CD spectrum of CT DNA is compared with that of DNA-bound [**2a**]Cl in Tris-HCl buffer (pH = 7.2). The experiment was performed at a molar ratio of r =15 (r = [DNA]/[**2a**$^+$]) at which fluorescence quenching of **2a**$^+$ by DNA was saturated (vide infra). The observed CD spectrum of the free CT DNA exhibits[30] a positive band at 275 nm due to base stacking and a negative band at 245 nm due to helicity of B-DNA. Figure 8 shows the CD spectra of free CT DNA, uncomplexed **2a**$^+$, and CT DNA-bound **2a**$^+$. Notably, the relative intensities of both the above bands of DNA increased due to addition of the binder. Moreover, the free triazinium cation (binder) has negligible contribution to the CD absorption region. The results thus confirm binding of the triazinium cation to DNA. It has been

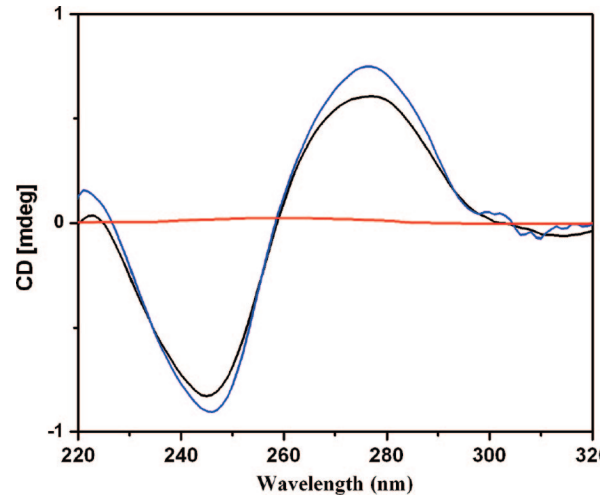

Figure 8. CD spectra of uncomplexed **2a**$^+$ (red), free CT DNA (black), and CT DNA in the presence of **2a**$^+$ (blue) at r = 15 in Tris-HCl, 50 mM NaCl buffer.

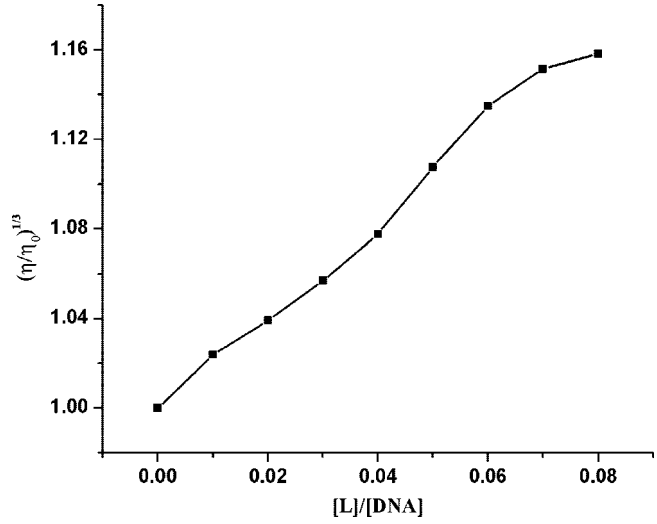

Figure 9. Effect of increasing amount of **2a**$^+$ on the relative viscosity of CT DNA in Tris-HCl, 50 mM NaCl buffer.

reported that the ruthenium complex of hqdppz ligand (hqdppz = 5,18-dihydroxynaphtho[2,3-*a*]dipyrido[3,2-*h*:2,3-*f*]phenazine) causes an increase[31] of intensities of both positive and negative bands of CT DNA due to intercalation. Final evidence in favor of possible intercalative binding of **2a**$^+$ was, however, achieved from the viscosity studies (see below).

Viscosity Measurements. To further clarify the nature of interaction between [**2a**]Cl and CT DNA, viscosity measurements were carried out. Upon binding, a DNA intercalator causes an increase in the viscosity of the DNA double helix due to its insertion between the DNA base pairs and consequently to the lengthening of the DNA double helix. In contrast, a partial and/or nonclassical intercalation could bend (or kink) the DNA helix, reducing the effective length and its viscosity.[32] The method is generally considered the least unambiguous to probe the mode of binding of a compound to DNA. The effect of [**2a**]Cl on viscosity of CT DNA is shown in Figure 9. The viscosity of DNA increased dramatically upon addition of [**2a**]Cl

(28) (a) Takeneka, S.; Ihara, T.; Takagi, M. *J. Chem. Soc., Chem. Commun.* **1990**, 1485. (b) Carter, M. T.; Rodriguez, M.; Bard, A. J. *J. Am. Chem. Soc.* **1989**, *111*, 8901.
(29) (a) Aslanoglu, M. *Anal. Sci.* **2006**, *22*, 439. (b) Hu, X.; Wang, Q.; He, P.; Fang, Y. *Anal. Sci.* **2002**, *18*, 645.
(30) Ivanov, V. I.; Minchenkova, L. E.; Schyolkina, A. K.; Poletayer, A. I. *Biopolymers* **1973**, *12*, 89.
(31) Maheswari, P. U.; Palaniandavar, M. *J. Inorg. Biochem.* **2004**, *98*, 219.

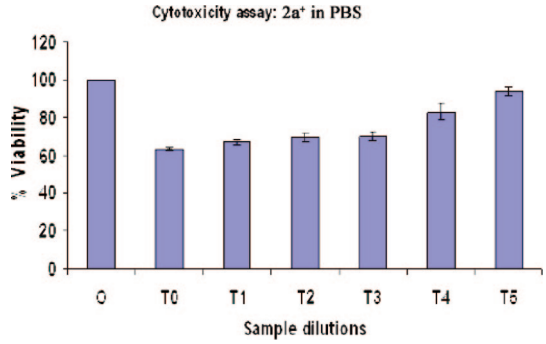

Figure 10. The effects of $\mathbf{2a}^+$ VERO cells' viability. Cells were treated for 30 h with the compound at the indicated concentrations. Cell viability was estimated by a MTT assay, as reported in the Experimental Section. Data are expressed as the percentage of viable cells with respect to untreated controls.

and is nearly linear at low concentration region. These results strongly indicate that the triazinium ion intercalated deeply into the DNA base pairs.

Cytotoxicity and Cellular Uptake. The cytotoxicity of $\mathbf{2a}^+$ against cancerous human epithelial cell lines (HeLa) and a noncancerous monkey kidney fibroblast cell (VERO) were studied using the MTT assay. The results of the cell cytotoxicity assay[33] indicate that there was no significant variation for the two different cell lines. The compound [**2a**]Cl exhibited significant potency at high concentration range, 1 mg/mL to 1 μg/mL. However, the % survival ratio increased with dilution. For example, at a low concentration, 0.1 μg/mL of $\mathbf{2a}^+$ has very little effect on the cells and may be considered to be nontoxic. The % viability with respect to the negative control is summarized in Figure 10. Cellular uptake studies[34] were also performed to ascertain whether the cytotoxicity results correlated with the cellular levels. The accumulation of $\mathbf{2a}^+$ was confirmed by FACS analysis of cellular dye uptake using VERO cells. The uptake level was found to be time-dependent and also dependent upon the dose of $\mathbf{2a}^+$. Notably, the uptake was found to be linear with respect to time (Supplementary Figure S9). In order to identify localization of $\mathbf{2a}^+$ in or near the cell nucleus, studies were undertaken using confocal microscopy. The experimental results (Figure 11) indicate clear localization of $\mathbf{2a}^+$ as green fluorescence mostly inside the nucleus. It has been known that DAPI stains the nucleus, producing blue fluorescence.

Conclusion and Scope

In this work, we have introduced a simple and one-pot synthesis of a family of flat triazinium cations $\mathbf{2a}^+$ having several useful chemical characteristics. The synthetic methodology is not only new but also has several distinct advantages over most of the available procedures. Both in vitro and ex vivo studies have confirmed that the compound [**2a**]Cl binds DNA strongly even in the nanogram range. Moreover, the compounds undergo reduction reversibly at low cathodic potentials (near –0.3 V vs SCE), producing stable free radicals. Estimated excited-state redox potentials of these are exceptionally high (ca. 2.0 V), which may be useful for the photo-induced oxidation of DNA. In this context, it may be relevant to add that the biomimetic approach of in vitro DNA damaging using chemical nucleases is a topic of interest for elucidating the genetic mechanisms of the natural enzymes involved in DNA scission, repair, and signal transduction. However, further studies are necessary to demonstrate the chemical nuclease activities of the present class of compounds. Our work in this area continues.

Experimental Section

Materials. *trans*-2-(Arylazo)pyridines were prepared by following the reported procedure.[14] Disodium salt of calf thymus DNA (highly polymerized) purchased from Sigma Aldrich was stored at 4 °C. **CAUTION:** Perchlorate salts of the compounds have to be handled with care and appropriate safety precautions. All other chemicals and solvents were of reagent grade and used as received.

Instrumentation. Perkin-Elmer Lambda 950 and Perkin-Elmer LS 55 spectrophotometers were used to record UV–vis and fluorescence spectra, respectively. Infrared spectra (KBr pellets) were recorded with a Shimadzu FTIR-8400S spectrophotometer. NMR spectra were recorded on a Bruker Avance 300 spectrometer, and $SiMe_4$ was used as the internal standard. A Perkin-Elmer 240C elemental analyzer was used to collect microanalytical data (C, H, N). ESI mass spectra were recorded on a micromass Q-TOF mass spectrometer (serial no. YA263). Electrochemical measurements were performed at 298 K under a dry nitrogen atmosphere on a

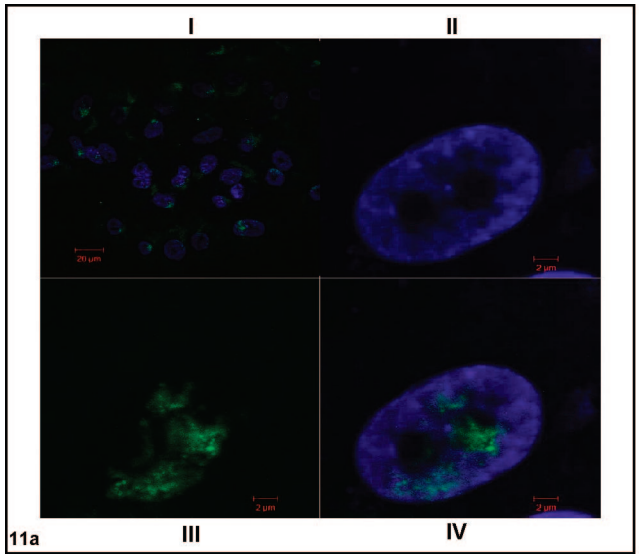

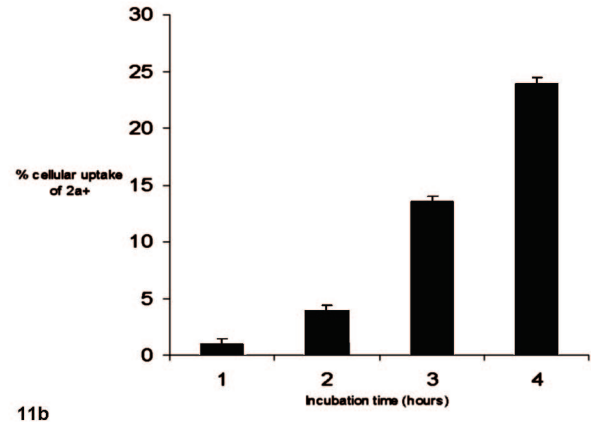

Figure 11. (a) Localization of $\mathbf{2a}^+$ in VERO cells: The confocal microscopic images show that most of the $\mathbf{2a}^+$ gets incorporated into the nucleus. **I** represent localization of $\mathbf{2a}^+$ at around the nucleus (green fluorescence); **II**, **III**, and **IV** represent the nucleus of a single cell stained with DAPI (blue fluoresence), $\mathbf{2a}^+$, and overlap of **II** and **III**, respectively. (b) Cellular uptake studies: % cellular uptake of $\mathbf{2a}^+$ by VERO cells with increasing time (h).

PC-controlled PAR model 273A electrochemistry system. A platinum disk (working) electrode, a platinum wire (auxiliary) electrode, and an aqueous saturated calomel reference electrode (SCE) were used in a three-electrode configuration. The $E_{1/2}$ for the ferrocenium−ferrocene couple under our experimental condition was 0.39 V. All potentials in this work are uncorrected for junction contribution. Circular dichroism spectra were recorded in a quartz cuvette of 1 mm path length with a Jasco J-815 spectropolarimeter. Viscosity measurements were conducted on an Ubbelodhe viscometer, immersed in a thermostated water bath maintained at 298 K.

Synthesis. The triazinium salts [**2a**]X were prepared following a general procedure by simply stirring a mixture of acetonitrile solution of *trans*-2-(arylazo)pyridine and HX (X = Cl, ClO_4, NO_3, and HSO_4). Details of a representative are given below.

Benzo[*e*]pyrido[2,1-*c*][1,2,4]triazin-11-ium Chloride. A mixture of *trans*-2-(phenylazo)pyridine (0.183 g, 1 mM) and an aqueous HCl solution (0.01 M) in acetonitrile was stirred for 5 days at room temperature. The initial orange color of the solution changed to light yellow during this period. On evaporation of the solvent, a yellow crude mass was obtained which was washed with chloroform thoroughly to remove unreacted *trans*-2-(phenylazo)pyridine. The crude product was then recrystallized by slow diffusion of toluene into the acetonitrile solution. Characterization data of the crystallized compound are as follows:

[2a]Cl ESI-MS: *m/z* 181.9 $[M]^+$. Anal. Calcd for $C_{11}H_8N_3Cl$: C, 60.7; H, 3.7; N, 19.31. Found: C, 60.81; H, 3.93; N, 19.54. ^{1}H NMR (D_2O): δ 10.15 (d, J = 6.66 Hz, 1H), 9.27 (d, J = 8.25 Hz, 1H), 9.06 (dd, J_1 = 8.13 Hz, J_2 = 8.52 Hz, 1H), 8.97 (d, J = 8.19 Hz, 1H), 8.92 (d, J = 8.76 Hz, 1H), 8.59 (dd, J_1 = 6.66 Hz, J_2 = 6.99 Hz, 1H), 8.48 (dd, J_1 = 7.98 Hz, J_2 = 8.04 Hz,1H), 8.32 (dd, J_1 = 7.71 Hz, J_2 = 7.77 Hz, 1H). ^{13}C NMR (D_2O): δ 146.4, 142.8, 141.9, 140.1, 134.1, 133.0, 132.8, 130.9, 129.9, 123.1, 116.5.

The other compounds listed in Chart 1 are prepared similarly using appropriate *trans*-2-(arylazo)pyridine and HX. Their characterization data are as follows.

[2a]ClO_4 ESI-MS: *m/z* 181.9 $[M]^+$. Anal. Calcd for $C_{11}H_8N_3ClO_4$: C, 46.91; H, 2.86; N, 14.92. Found: C, 46.93; H, 2.85; N, 14.91. ^{1}H NMR (CD_3CN): δ 9.92 (d, J = 6.6 Hz, 1H), 9.25 (d, J = 8.16 Hz, 1H), 9.06–9.03 (m, 2H), 8.81 (d, J = 8.88 Hz, 1H), 8.55–8.53 (m, 2H), 8.34 (dd, J_1 = 8.01 Hz, J_2 = 7.62 Hz, 1H).

[2a]NO_3 ESI-MS: *m/z* 181.9 $[M]^+$. Anal. Calcd for $C_{11}H_8N_4O_3$: C, 54.1; H, 3.3; N, 22.94. Found: C, 53.92; H, 3.44; N, 23.13. ^{1}H NMR (CD_3CN): δ 10.03 (d, J = 6.36 Hz, 1H), 9.25 (d, J = 8.22 Hz, 1H), 9.06–9.00 (m, 2H), 8.88 (d, J = 8.61 Hz, 1H), 8.58–8.46 (m, 2H), 8.35 (dd, J_1 = 7.77 Hz, J_2 = 7.53 Hz, 1H).

[2b]Cl ESI-MS: *m/* 195.9 $[M]^+$. Anal. Calcd for $C_{12}H_{10}N_3Cl$: C, 62.21; H, 4.35; N, 18.14. Found: C, 62.15; H, 4.37; N, 17.94. ^{1}H NMR (CD_3CN): δ 9.88 (d, J = 6.6 Hz, 1H), 9.21 (d, J = 8.28 Hz, 1H), 8.98 (dd, J_1 = 7.52 Hz, J_2 = 7.57 Hz, 1H), 8.81 (s, 1H), 8.71 (d, J = 8.88 Hz, 1H), 8.52 (dd, J_1 = 6.59 Hz, J_2 = 6.72 Hz, 1H), 8.32 (d, J = 8.81 Hz, 1H), 2.76 (s, 3H).

[2c]Cl ESI-MS: *m/* 196.1 $[M]^+$. Anal. Calcd for $C_{12}H_{10}N_3Cl$: C, 62.21; H, 4.35; N, 18.14. Found: C, 62.05; H, 4.24; N, 18.31. ^{1}H NMR (CD_3CN): δ 10.04 (d, J = 6.70 Hz, 1H), 9.18 (d, J = 8.22 Hz, 1H), 8.97 (dd, J_1 = 7.74 Hz, J_2 = 7.90 Hz, 1H), 8.88 (d, J = 8.40 Hz, 1H), 8.83 (s, 1H), 8.52 (dd, J_1 = 6.51 Hz, J_2 = 7.42 Hz, 1H), 8.18 (d, J = 8.34 Hz, 1H), 2.82 (s, 3H).

[2d]Cl ESI-MS: *m/z* 212.1 $[M]^+$. Anal. Calcd for $C_{12}H_{10}N_3ClO$: C, 58.19; H, 4.07; N, 16.96. Found: C, 58.24; H, 4.32; N, 16.73. ^{1}H NMR (CD_3CN): δ 9.90 (d, J = 6.65 Hz, 1H), 9.08 (d, J = 8.17 Hz, 1H), 8.93–8.86 (m, 2H), 8.44 (dd, J_1 = 5.75 Hz, J_2 = 6.63 Hz, 1H), 8.13 (s, 1H), 7.89 (d, J = 9.29 Hz, 1H), 4.2219 (s, 3H).

[2e]Cl ESI-MS: *m/z* 216.1 $[M]^+$. Anal. Calcd for $C_{11}H_7N_3Cl_2$: C, 52.4; H, 2.79; N, 16.67. Found: C, 52.26; H, 3.16; N, 16.87. ^{1}H NMR (CD_3CN): δ 9.91 (d, J = 6.45 Hz, 1H), 9.31 (d, J = 7.99 Hz, 1H), 9.09 (dd, J_1 = 7.66 Hz, J_2 = 7.67 Hz, 1H), 8.75–8.72 (m, 2H), 8.58 (dd, J_1 = 7.2 Hz, J_2 = 7.32 Hz, 1H), 8.41 (d, J = 6.33, 1H).

[2f]Cl ESI-MS: *m/z* 216.1 $[M]^+$. Anal. Calcd for $C_{11}H_7N_3Cl_2$: C, 52.41; H, 2.79; N, 16.67. Found: C, 52.55; H, 3.23; N, 16.57. ^{1}H NMR (CD_3CN): δ 9.82 (d, J = 6.62 Hz, 1H), 9.25 (d, J = 8.26 Hz, 1H), 9.06 (dd, J_1 = 7.83 Hz, J_2 = 7.94 Hz, 1H), 8.97 (d, J = 7.62, 1H), 8.93 (s, 1H), 8.57 (dd, J_1 = 7.66 Hz, J_2 = 7.67 Hz, 1H), 8.33 (d, J = 8.73 Hz, 1H).

[2g]Cl ESI-MS: *m/z* 260.1 $[M]^+$. Anal. Calcd for $C_{11}H_7N_3ClBr$: C, 44.55; H, 2.37; N, 14.17, Found: C, 44.92; H, 2.86; N, 13.89. ^{1}H NMR (CD_3CN): δ 9.85 (d, J = 5.19 Hz, 1H), 9.24 (d, J = 7.05 Hz, 1H), 9.10–9.06 (m, 2H), 8.88 (d, J = 7.82, 1H), 8.57 (dd, J_1 = 5.82 Hz, J_2 = 6.27 Hz, 1H), 8.47 (d, J = 7.46 Hz, 1H).

DNA Binding Experiments. The concentration of CT DNA was determined[35] from the absorption intensity at 260 nm with a molar extinction coefficient of 6600 M^{-1} cm^{-1}. The solution was stored at 4 °C and was used after no more than 4 days. Doubly distilled water was used to prepare the buffer solution. Fluorescence measurements[22a] were carried out by keeping the concentration of triazinium ion constant (20 μM) and varying the concentration of calf thymus (CT) DNA from 20 to 320 μM in Tris-HCl/NaCl buffer (pH 7.2). The solutions were excited at 340 nm, and the fluorescence spectra were recorded between 360 and 900 nm. The quenching efficiency is evaluated by the Stern−Volmer constant K_{SV}

$$I_0/I = 1 + K_{SV}[Q] \quad (3)$$

where I_0 and I are the emission intensities in the absence and the presence of DNA, [Q] is the concentration of DNA. The relative binding of the **2a**$^+$ ion to CT DNA was studied using the fluorescence spectral method with an ethidium-bromide-bound (EB-bound) CT DNA solution in Tris-HCl/NaCl buffer (pH 7.2). Fluorescence intensities at 600 nm (510 nm excitation) were measured at different **2a**$^+$ ion concentrations. Addition of the triazinium ion showed a reduction in emission intensity. The relative binding of the triazinium to CT DNA (K_{app}) was determined following the reported procedure.[24] Ferrocyanide-induced emission quenching of the triazinium compound was performed keeping the concentration of **2a**$^+$ constant (20 μM) in the absence and presence of DNA ([DNA]/[**2a**$^+$] = 10), and the concentration of ferrocyanide was varied between 0.02 and 0.08 mM. DNA melting experiments were carried out by monitoring the absorbance (260 nm) of CT DNA at various temperatures starting from 50 °C in the absence and presence of the triazinium ion at r = 10 ratio (r = [DNA]/[**2a**$^+$]) using a Peltier system attached to UV–vis spectrophotometer with an increment of 1 °C/4 min. In circular dichroic spectra, the concentration of **2a**$^+$ was 6.6 μM (uncomplexed), DNA was 100 μM (free), and in case of DNA-bound **2a**$^+$, the r value was 15 (r = [DNA]/[**2a**$^+$]). Viscometric titrations were performed by the addition of aliquots of the **2a**$^+$ solution into a constant concentration of DNA solution.

Gel Electrophoresis. The interaction between **2a**$^+$ and DNA was studied using agarose gel electrophoresis technique. In agarose gel electrophoresis, **2a**$^+$ was used instead of ethidium bromide during the electrophoresis in 0.8% agarose in 0.5X TBE buffer (45 mM Tris-borate, 1 mM EDTA, pH 8.0). The final concentration of the **2a**$^+$ in the gel was 0.5 μg/mL. The DNA was visualized under a trans-illuminator (Bangalore Genei, India). All the agarose gel pictures were captured in the GelDoc system (BioRad Laboratories Inc., Herculis, CA).

(32) (a) Waring, M. J. *J. Mol. Biol.* **1970**, *54*, 247. (b) Veal, J. M.; Rill, R. L. *Biochemistry* **1991**, *30*, 1132. (c) Satyanarayana, S.; Dabrowiak, J. C.; Chaires, J. B. *Biochemistry* **1992**, *31*, 9319. (d) Satyanarayana, S.; Dabrowiak, J. C.; Chaires, J. B. *Biochemistry* **1993**, *32*, 2573.
(33) Mosmann, T. *J. Immuno. Methods* **1983**, *65*, 55.
(34) (a) Prathihar, J. L.; Shee, B.; Pattanayak, P.; Patra, D.; Bhattacharyya, A.; Puranik, V. G.; Hung, C. H.; Chattopadhyay, S. *Eur. J. Inorg. Chem.* **2007**, *27*, 4272. (b) Ma, D.-L.; Che, C.-M.; Situ, F.-M.; Yang, M.; Wong, K.-Y *Inorg. Chem.* **2007**, *46*, 740.
(35) Reichmann, M. E.; Rice, S. A.; Thomas, C. A.; Doty, P. *J. Am. Chem. Soc.* **1954**, *76*, 3047.

Cell Cytotoxicity Test and Cellular Uptake Studies. Human epithelial (HeLa) cells and monkey kidney fibroblast (VERO) cells were maintained in DMEM media supplemented with 5% (v/v) calf serum, 2 mmol/L glutamine, and 1% (v/v) penicillin (streptomycin). Cells (T-25 flask) were cultured at 37 °C in a humid atmosphere containing 5% CO_2 and subcultured every 2–3 days. Cells were harvested with trypsin, and a suspension containing 2×10^5 cells per mL was prepared. This assay was performed in a 96-well, flat-bottomed, γ-irradiated, microliter plates with lids. Filter sterilized (0.22 μm), PBS soluble **2a**$^+$ (1 mg/mL) (50 μL) was serially diluted 10^5-fold. Negative controls (50 μL phosphate buffer saline) and positive controls (50 μL Triton X-100) were included. Cells were grown in the wells for 24 h up to 70–80% confluence. The wells were then inoculated aseptically with 50 μL of different dilutions of the samples, negative controls, and the positive controls, and the plates were incubated at 37 °C in a humid atmosphere containing 5% CO_2 for 30 h. After the incubation period, 50 μL of an aqueous solution of MTT (3-(4,5-dimethylthiazol-2-yl)-2,5-diphenyl tetrazonium bromide) (2 mg/mL) was added to each well, and the plates were incubated for a further 4 h at 37 °C in a humid atmosphere containing 5% CO_2. After this time, the liquid medium in the wells was removed, 200 μL of dimethyl sulfoxide (DMSO) was added to each well, and the absorbance at 450 nm was determined in a microplate reader. The toxic effect of **2a**$^+$ on the HeLa cell line was calculated from the following (eq 4)

$$[1 - (OD_{\text{negative control}}/OD_{\text{test}})] \times 100 \quad (4)$$

Samples were considered to be toxic if the optical density of the test well was >20% less than that detected in the negative control wells.

Cellular uptake experiments were conducted according to a literature method with some modifications. VERO cells (5.4×10^4 cells) were seeded in 60 mm tissue culture dishes containing culture medium (2 mL/well) and incubated at 37 °C in an atmosphere of 5% CO_2/95% air for 24 h. The culture medium was removed and replaced by a medium containing 50 μL of **2a**$^+$ (concentration 1 mg/mL). After exposure to **2a**$^+$ for 2, 4, and 6 h, the medium was removed and the cell monolayer was washed 4 times with ice-cold PBS. Cells were then scraped off the culture dish. Samples were suspended in 1 mL of PBS and applied to the FACS analyzer (BD Biosciences) against proper control cells.

Confocal Microscopy. VERO cells (5.4×10^4 cells) were seeded in 60 mm tissue culture dishes containing culture medium (2 mL/well) and incubated at 37 °C in an atmosphere of 5% CO_2/95% air for 24 h. The culture medium was removed and replaced by a medium containing 50 μL of **2a**$^+$ (concentration 1 mg/mL) and then kept for 4 h. The cells were then fixed with 4% paraformaldehyde, washed with PBS, permeabilized with 0.5% Triton X-100 in PBS for 10 min, and then examined under a confocal microscope (Zeiss, LSM510 META, at ×63 magnification, oil immersion). In another set, cells were first fixed using a similar procedure and then treated with **2a**$^+$ and then examined under a confocal microscope. In treated and untreated cells, the nuclei were counterstained with DAPI.

Crystallography. Suitable X-ray quality crystals ($0.30 \times 0.10 \times 0.06$) of [**2a**]$CF_3SO_3$ are obtained by slow diffusion of toluene into an acetonitrile solution of the compound. The data were collected on a Nonius Kappa CCD detector, equipped with Mo Kα radiation ($\lambda = 0.71073$ Å), and were corrected for Lorentz polarization effects. A total of 5069 reflections were collected, out of which 2996 were unique ($R_{\text{int}} = 0.044$) and were used in subsequent analysis. The structure was solved by employing the SHELXS-97 program package[36a] and refined by full-matrix least-squares based on F^2 (SHELXL-97).[36b] All hydrogen atoms were added in calculated positions. Crystallographic data of [**2a**]CF_3SO_3 are collected in Table 4.

Table 4. Crystallographic Data for [**2a**]CF_3SO_3

empirical formula	$C_{12}H_8N_3F_3O_3S$
formula weight	331.28
temperature, K	150(2)
crystal system	monoclinic
space group	*P*21/*c*
a, Å	12.9900(9)
b, Å	16.0879(13)
c, Å	6.1202(4)
α, degree	90
β, degree	92.373(5)
γ, degree	90
V, Å^3	1277.91(16)
$D_{\text{calc.}}$, gm/ cm^3	1.722
Z	4
crystal dimensions	$0.30 \times 0.10 \times 0.06$
θ range for data collection, degree	3.0–27.9
GOF	1.168
total reflections collected	5069
unique reflections	2996
final *R* indices [$I > 2\sigma(I)$]	$R_1 = 0.0772$ $wR_2 = 0.1673$

Acknowledgment. Dedicated to Professor Animesh Chakravorty, IACS, Kolkata. The research was supported by the Department of Science and Technology, India (Project SR/S1/IC-24/2006). Crystallography was performed at the DST-funded National Single Crystal Diffractometer Facility at the Department of Inorganic Chemistry, IACS. We are thankful to Professor Kankan Bhattacharya for Lifetime measurement of one of the reference compounds at the DST sponsored Femtosecond facility at IACS. We are also thankful to Dr. Kumaresh Ghosh for helpful discussions. M.S. and M.P. are thankful to the CSIR for fellowship support. Constructive suggestions of the reviewers were helpful at the revision stage.

Supporting Information Available: X-ray crystallographic files in CIF format for [**2a**]CF_3SO_3; ^{1}H NMR spectrum of [**2b**]Cl (S1), ^{13}C NMR spectrum of [**2a**]Cl (S2), an ORTEP and atom numbering scheme of [**2a**]CF_3SO_3 (S3), cyclic voltammogram of [**2f**]Cl (S4), Hammett's plot (S5), gel electrophoresis (S6), emission spectra of DNA-bound EtBr with [**2a**]Cl (S7), DNA melting curve (S8), cellular uptakes studies (S9). This material is available free of charge via the Internet at http://pubs.acs.org.

JA710211U

(36) (a) Sheldrick, G. M. *Acta Crystallogr., Sect. A* **1990**, *46*, 467. (b) Sheldrick, G. M. *SHELXL 97. Program for the refinement of crystal structures*; University of Göttingen; Göttingen, Germany, 1997.